Computer Fraud and Security
ISSN (online): 1873-7056

Tourism Demand Forecasting based on Adaptive Neural Network Technology in Business Intelligence

Jun Li
Department of Tourism Management, Zhengzhou Tourism College, Zhengzhou, Henan, China

Abstract:

In order to improve the effect of demand forecasting, this paper combines the adaptive neural network technology to construct a demand forecasting model, and proposes an adaptive fault-tolerant PI control strategy for multiple-input and multiple-output systems. In order to verify the effectiveness and stability of the designed adaptive fault-tolerant PI control strategy, this paper uses an iterative algorithm to improve the tracking control accuracy. Moreover, this paper integrates temporal geography with the theory of probabilistic temporal geography, system analysis theory, and tourist flow space-time bayonet theory to propose a research framework for forecasting tourist flow spatio-temporal bayonet based on the WITNESS simulation system. The research shows that the tourism demand forecasting model based on adaptive neural network technology proposed in this paper has good tourism demand forecasting effect, and has a certain effect on promoting the development of tourism.

Keywords: business intelligence; adaptive neural network; tourism demand; forecast

1 INTRODUCTION

With the development of the times, tourism has become an important economic industry in today's world, and tourism has become an indispensable part of modern people's daily life. However, many travel and hospitality products cannot be stored for future use, such as vacant hotel rooms, unsold event tickets and unconsumed merchandise. Therefore, accurate tourism demand forecasts can help to develop strategies related to tourism development to make informed decisions on issues such as infrastructure development and accommodation site planning. Moreover, accurate tourism demand forecast is crucial to the development of tourism economy.

The forecasting methods of tourism demand are mainly divided into two categories: traditional quantitative and qualitative methods and artificial intelligence. Quantitative forecasting mainly relies on the establishment of quantitative forecasting models, and is currently a widely used tourism demand forecasting method [1]. The common methods include time series methods and econometric methods. Artificial intelligence methods include grey theory, rough set theory, neural network model, etc. Traditional quantitative and qualitative research methods need to meet many constraints when using mathematical algorithms, and need to make a variety of assumptions in the modeling process, so there is a large deviation between the predicted results and the real results [2]. However, AI methods often require large amounts of data, which is not always possible in real life. Although these methods can reflect the general trend of changes in tourism demand, it is difficult to accurately predict using the above models in the absence of data and uncertainties, so it is necessary to try to use a new model for forecast [3].

The accurate forecast of tourism demand can greatly improve the quantitative level of tourism economy, provide theoretical basis for tourism market development, and solve the problems existing in tourism in time. For a long time, the forecasting methods of tourism demand are mainly divided into two categories: traditional quantitative and qualitative methods and artificial intelligence. Traditional quantitative and qualitative research methods need to meet many constraints when using mathematical algorithms, and they need to make a variety of assumptions in the modeling process, so the predicted results have a large deviation from the real results; and some methods of artificial intelligence usually require a large number of data, which is not always possible in real life. Although these methods can reflect the general trend of changes in tourism demand, it is difficult to use the above models to make accurate predictions in the absence of data and uncertainties. It is necessary to try to use new models and methods to make predictions.

This paper combines the adaptive neural network technology to construct a demand forecasting model, which provides an auxiliary system for the development of modern tourism.

2 RELATED WORK

From the perspective of research on factors affecting tourism demand, foreign scholars have conducted many studies on the rapid growth of tourism demand caused by different factors. Literature [4] mainly studies the income elasticity and price elasticity of tourism demand on international tourism demand; Literature [5] analyzes the influence of factors such as income, price, time, and population on tourism demand by establishing a model. From the perspective of demand forecasting methods, it mainly focuses on quantitative research. The main models include time series forecasting models, regression forecasting models, and gravity forecasting models. Literature [6] uses a time series model to forecast tourism demand in Australia, including moving average method, seasonal autoregressive model, exponential smoothing method, multiple regression model, etc.; Literature [7] uses regression model to segment different tourism segments. The tourism spending of the market is analyzed by the difference between tourist source and destination. Literature [8] adopts the vector autoregressive model, the mixed model of the measurement autoregression and the fuzzy model, etc.

There are also more and more scholars studying the influencing factors of tourism demand forecasting. Literature [9] uses artificial neural network model to study the influencing factors of residents' tourism demand, which are basically divided into income, the proportion of tourism consumption to total income, and tourism supply. Intensity, and traffic conditions are four major factors. Literature [10] uses time series model and grey relational analysis model to determine the main factors of tourism demand as living standard, cultural level, traffic conditions and so on.

At present, the main forecasting methods include artificial neural network, SARIMA model, multiple regression analysis, exponential smoothing method, curve fitting method, grey forecasting model, EGARCH model, etc. [11]. Regarding tourism demand forecasting, the literature mostly focuses on the determination of tourism demand factors and the description of tourism spatial distribution and behavior. There are few studies on tourism demand forecasting in a specific region. Literature [12] uses a variety of forecasting models to find the most suitable model for Hangzhou tourism demand forecasting. And considering the difference of the model, the prediction is divided into two cases: without considering the influencing factors and considering the influencing factors.

The causal analysis is mainly to obtain the statistical conclusions of the regression accuracy and significance, and at the same time, it can also establish a model between the demand data and various influencing factors to realize the modeling. As long as the model and data used are the same, a unique result can be calculated by standard statistical methods, but when interpreting the chart, the interpretation of the relationship between the data can vary from person to person, and the fit drawn by the analysis is different. The curves may also be different [13]. Non-causal analysis mainly refers to time series analysis, and its advantage is that it is more effective in analyzing the relationship between the present, the past, and the future, as well as the relationship between the future results and various factors in the past and present. At the same time, the data processing is not very complicated. But it only performs well when the forecast is stable and continues steadily in time, and it is not suitable for long-term forecasting. And the time series model has an obvious disadvantage, because its model only makes judgments on the future based on past data, so it does not consider the reasons for tourists' travel demand and various interference factors, so the time series model is not suitable for tourism suppliers. In-depth demand analysis cannot bring more information to tourism managers and tourism business operators [14]. The gray model is a method used when the original data has a certain unclear nature, so its requirements for the original data are relatively loose, and the comprehensive situation of multiple influencing factors can be considered at the same time, and the conclusions given are more stable and more realistic. , but due to unknown information in the original data, there is often a large deviation. The regression model is suitable for long-term prediction, and there are many classifications of regression models, which are suitable for various types of prediction models, but the requirements for original data are relatively high, and the level of knowledge is required to be high. It is also often used by scholars for tourism. method of demand forecasting [15].

Literature [16] used the econometric model OLS, ordinary least squares and SUR surface uncorrelated regression to predict tourism demand, and compared the accuracy of the model results. Literature [17] used data for modeling, and the prediction results were compared and analyzed by MAPE, MSE, RMSPE, and MAD, and it was found that the exponential smoothing method and the autoregressive moving average method had relatively good effects. The results of the literature [18] show that the latest econometric model is more accurate than the least squares regression model, but still worse than the unchanged model and the time series model.

3 ADAPTIVE NEURAL NETWORK ALGORITHM

Differentiating over time and substituting, the following tracking error model can be obtained:

$$\begin{aligned}\dot{\boldsymbol{Z}} &= \omega_1(\boldsymbol{X}_2-\boldsymbol{X}_2^*)+\omega_2(\boldsymbol{X}_3-\boldsymbol{X}_3^*)+\cdots\\ &\quad+\omega_{q-1}\left(\boldsymbol{X}_q-\boldsymbol{X}_q^*\right)+\left(\dot{\boldsymbol{X}}_q-\dot{\boldsymbol{X}}_q^*\right)\\ &=\mathbf{G}(\overline{\boldsymbol{X}},t)\boldsymbol{\rho}\left(t_\rho,t\right)\boldsymbol{u}+f(\overline{\boldsymbol{X}},t)+\boldsymbol{G}(\overline{\boldsymbol{X}},t)\boldsymbol{u}_r(t_r,t)\\ &\quad+\omega_1(\boldsymbol{X}_2-\boldsymbol{X}_2^*)+\omega_2(\boldsymbol{X}_3-\boldsymbol{X}_3^*)+\cdots\\ &\quad+\omega_{q-1}\left(\boldsymbol{X}_q-\boldsymbol{X}_q^*\right)-\dot{\boldsymbol{X}}_q^*\\ &=\mathbf{G}(\overline{\boldsymbol{X}},t)\boldsymbol{\rho}\left(t_\rho,t\right)\boldsymbol{u}+\boldsymbol{L}\end{aligned}\quad(1)$$

Among them,

$$\begin{aligned}\boldsymbol{L}&=\boldsymbol{f}(\overline{\boldsymbol{X}},t)+\boldsymbol{G}(\overline{\boldsymbol{X}},t)\boldsymbol{u}_r(t_r,t)+\omega_1(\boldsymbol{X}_2-\boldsymbol{X}_2^*)\\ &\quad+\omega_2(\boldsymbol{X}_3-\boldsymbol{X}_3^*)+\cdots+\omega_{q-1}\left(\boldsymbol{X}_q-\boldsymbol{X}_q^*\right)-\dot{\boldsymbol{X}}_q^*\end{aligned}\quad(2)$$

The corresponding adaptive fault-tolerant control PI strategy is proposed below for different actuator failure modes.

First, the failure case of partial failure of the actuator is considered. In this case, the actuator loses some efficiency, but still can work and output torque. In order to facilitate the design of the controller, filter variables are introduced:

$$\boldsymbol{S}=\boldsymbol{Z}+\beta\int_0^t\boldsymbol{Z}\,d\tau\quad(3)$$

Among them, $\beta>0$ is a parameter that can be freely selected by the designer.

For the above variables, it can also be shown that if t approaches infinity, S approaches 0. Then, as time goes to infinity, $\boldsymbol{Z}$ and $\int_0^t\boldsymbol{Z}\,\boldsymbol{d\tau}$ asymptotically tend to 0 at the same rate. The goal of control is thus transformed into designing a PI controller such that S is eventually consistently bounded.

The proposed PI control strategy has the following form:

$$\boldsymbol{u}=-\frac{A^T}{\|A\|}(k_{P1}+\Delta k_{P1}(t))\boldsymbol{Z}(t)-\frac{A^T}{\|A\|}(k_{I1}+\Delta k_{I1}(t))\int_0^t\boldsymbol{Z}\,(t)d\tau\quad(4)$$

The constant proportional gain $k_{P1}>0$ and the constant integral gain $k_{I1}=\beta k_{P1}$ are linked by the parameter β, which simplifies the process of gain adjustment and stability analysis. The time-varying proportional gain Δk_{P1} and integral gain Δk_{I1} are continuously adjusted and updated by the following algorithms[19]:

$$\Delta k_{P1}(t)=\sigma_1\hat{c}\psi^2,\Delta k_{I1}(t)=\beta\Delta k_{P1}(t)\quad(5)$$

Among them,

$$\dot{\hat{c}}=-\sigma_0\hat{c}+\sigma_1\psi^2\|\boldsymbol{S}\|^2,\hat{c}(0)\geq 0\quad(6)$$

$c=a^2$will be mentioned in a later article. $\hat{c}$is an estimate of the parameter c, and $\sigma_0>0$ and $\sigma_1>0$ are also parameters chosen by the designer.

Certification:

Applying the filter variable S defined by formula (3), formula (4) can be expressed in the following form:

$$\boldsymbol{u}=-\frac{A^T}{\|A\|}(k_{P1}+\Delta k_{P1})\boldsymbol{S}\quad(7)$$

By differentiating the filter variable S, we obtain:

$$\begin{aligned}\dot{\boldsymbol{S}}&=\dot{\boldsymbol{Z}}+\beta\boldsymbol{Z}\\ &=\mathbf{AM\rho u}+\mathbf{L}+\beta\mathbf{Z}\end{aligned}\quad(8)$$

The closed-loop system stability proof is performed when considering the Lyapunov function of the form:

$$V_1 = \frac{1}{2}\boldsymbol{S}^T\boldsymbol{S} + \frac{1}{2\mu}\tilde{c}^2 \quad (9)$$

Among them, $\tilde{c} = c - \mu\hat{c}$ is the unknown parameter estimation error. Taking the derivation of the above formula, we can obtain:

$$\begin{aligned}\dot{V}_1 &= \boldsymbol{S}^T\dot{\boldsymbol{S}} + \frac{1}{\mu}\tilde{c}\dot{\tilde{c}} \\ &= \boldsymbol{S}^T(\boldsymbol{Gu} + \boldsymbol{L} + \beta\boldsymbol{Z}) + \frac{1}{\mu}\tilde{c}(\dot{c} - v\dot{\hat{c}}) \\ &= -\frac{k_{P1}+\Delta k_{P1}}{\|\boldsymbol{A}\|}\boldsymbol{S}^T\boldsymbol{AM\rho A}^T\boldsymbol{S} + \boldsymbol{S}^T(\boldsymbol{L} + \beta\boldsymbol{Z}) - \tilde{c}\dot{\tilde{c}} \quad (10)\end{aligned}$$

Further, we can obtain:

$$\begin{aligned}&-\frac{k_{P1}+\Delta k_{P1}}{\|\boldsymbol{A}\|}\boldsymbol{S}^T\boldsymbol{AM\rho A}^T\boldsymbol{S} \\ &= -\frac{k_{P1}+\Delta k_{P1}}{\|\boldsymbol{A}\|}\boldsymbol{S}^T\left[\begin{matrix}\dfrac{\boldsymbol{AM\rho A}^T + (\boldsymbol{AM\rho A}^T)^T}{2} \\ + \dfrac{\boldsymbol{AM\rho A}^T + (\boldsymbol{AM\rho A}^T)^T}{2}\end{matrix}\right]\boldsymbol{S} \\ &= -\frac{k_{P1}+\Delta k_{P1}}{\|\boldsymbol{A}\|}\boldsymbol{S}^T\frac{\boldsymbol{AM\rho A}^T - (\boldsymbol{AM\rho A}^T)^T}{2}\Bigg]\boldsymbol{S} \\ &\le -(k_{P1}+\Delta k_{P1}) = \mu\|\boldsymbol{S}\|^2 \\ &= -k_{P1}\mu\|\boldsymbol{S}\|^2 - \sigma_1\mu\hat{c}\psi^2\|\boldsymbol{S}\|^2 \quad (11)\end{aligned}$$

It should be noted that the above formula applies the orthogonality of antisymmetric matrices:

$$\boldsymbol{S}^T\left[\frac{\boldsymbol{AM\rho A}^T - (\boldsymbol{AM\rho A}^T)^T}{2}\right]\boldsymbol{S} \equiv 0 \quad (12)$$

Under the assumptions, we obtain:

$$\begin{aligned}\|\boldsymbol{L} + \beta\boldsymbol{Z}\| &\le a_F F(\cdot) + \overline{gu}_r + \omega_1\|\boldsymbol{X}_2\| + \omega_1\|\boldsymbol{X}_2^*\| + \cdots \\ &\quad + \omega_{q-1}\|\boldsymbol{X}_q\| + \omega_{q-1}\|\boldsymbol{X}_q^*\| + \beta\|\boldsymbol{Z}\| \\ &\le a\psi(\cdot) \quad (13)\end{aligned}$$

Among them,

$$\begin{aligned}&a = max\{a_F, \overline{gu}_r, \omega_1, \omega_1\|\boldsymbol{X}_2^*\|, \cdots, \omega_{q-1}, \omega_{q-1}\|\boldsymbol{X}_q^*\|, \beta\} \\ &\psi(\cdot) = F(\cdot) + q + \|\boldsymbol{Z}\| + \|\boldsymbol{X}_2\| + \|\boldsymbol{X}_3\| + \cdots + \|\boldsymbol{X}_q\| \quad (14)\end{aligned}$$

Among them, a is an unknown constant and $\psi(\cdot)$is a computable function.

At this time, according to formulas (13) and (14), we get:

$$\boldsymbol{S}^T(\boldsymbol{L} + \beta\boldsymbol{Z}) \le a\psi\|\boldsymbol{S}\| \le \frac{1}{4\sigma_1} + \sigma_1 c\psi^2\|\boldsymbol{S}\|^2 \quad (15)$$

Among them, $c = a^2$ is mentioned above.

From formulas (10)-(15), we can get:

$$\begin{aligned}\dot{V}_1 &\le -k_{P1}\mu\|\boldsymbol{S}\|^2 - \sigma_1\mu\hat{c}\psi^2\|\boldsymbol{S}\|^2 \\ &\quad + \frac{1}{4\sigma_1} + \sigma_1 c\psi^2\|\boldsymbol{S}\|^2 + \sigma_0\tilde{c}\hat{c} - \sigma_1\tilde{c}\psi^2\|\boldsymbol{S}\|^2 \\ &= -k_{P1}\mu\|\boldsymbol{S}\|^2 + \sigma_1(c - \mu\hat{c})\psi^2\|\boldsymbol{S}\|^2 - \sigma_1\tilde{c}\psi^2\|\boldsymbol{S}\|^2 + \frac{1}{4\sigma_1} + \sigma_0\tilde{c}\hat{c} \\ &= k_{P1}\mu\|\boldsymbol{S}\|^2 + \frac{1}{4\sigma_1} + \sigma_0\tilde{c}\tilde{c} \quad (16)\end{aligned}$$

In the above formula, $\sigma_0\tilde{c}\hat{c}$ satisfies the following formula:

$$\begin{aligned}
\sigma_0\tilde{c}\hat{c} &= \sigma_0\tilde{c}\frac{1}{\mu}(c-\tilde{c}) \\
&\le \frac{\sigma_0}{\mu}\tilde{c}c - \frac{\sigma_0}{\mu}\tilde{c}^2 \\
&\le \frac{\sigma_0}{\mu}\left(\frac{1}{2}\tilde{c}^2 + \frac{1}{2}c^2 - \tilde{c}^2\right) \\
&= \frac{\sigma_0}{2\mu}c^2 - \frac{\sigma_0}{2\mu}\hat{c}^2 \quad (17)
\end{aligned}$$

Finally, we get:

$$\begin{aligned}
\dot{V}_1 &\le -k_{P1}\mu\|\boldsymbol{S}\|^2 - \frac{\sigma_0}{2\mu}\tilde{c}^2 + \frac{1}{4\sigma_1} + \frac{\sigma_0}{2\mu}c^2 \\
&\le -l_1V_1 + l_2 \quad (18)
\end{aligned}$$

Among them,

$$l_1 = min\{2k_{P1}\mu, \sigma_0\}, l_2 = \frac{1}{4\sigma_1} + \frac{\sigma_0}{2\mu}c^2 \quad (19)$$

Formula (18) can be further expressed as:

$$\dot{V}_1 \le -k_{P1}\mu\|\boldsymbol{S}\|^2 + l_2 \quad (20)$$

This shows that if $\|\boldsymbol{S}\| > \sqrt{\frac{l_2+\eta_1}{k_{P1}\mu}}$ ($\eta_1 > 0$ is a small constant), there is $\dot{V}_1 < 0$. Therefore, $\|\boldsymbol{S}\|$will enter the compact set[20].

$$\Omega_1 = \left\{\|\boldsymbol{S}\| \middle| \|\boldsymbol{S}\| \le \sqrt{\frac{l_2+\eta_1}{k_{P1}\mu}}\right\} \quad (21)$$

It is further shown that $\boldsymbol{S} \in \ell_\infty$ is eventually uniformly bounded, so the generalized tracking error $\boldsymbol{Z} \in \ell_\infty$ also satisfies the eventually uniformly bounded condition. $\boldsymbol{X} \in \ell_\infty$ can be guaranteed. From this, the stability of the adaptive PI control strategy in the case of partial actuator failure is demonstrated.

So far, the steps of adaptive PI control can be given, and its algorithm block diagram is shown in Figure 1:

(1) The algorithm sets the parameter σ_0、σ_1、ω_1、β、k_{P1}, and gives the initial values $\hat{c}(0)$、$\boldsymbol{X}(0)$ and $\dot{\boldsymbol{X}}(0)$;

(2) The algorithm calculates $\boldsymbol{Z}$、$\boldsymbol{S}$、ψ、$\hat{c}$ and obtainsΔk_{P1} and Δk_{I1};

(3) The algorithm calculates the system input $\boldsymbol{u}$ according to the control law (4);

(4) The algorithm obtains the state quantities $\boldsymbol{X}$ and $\dot{\boldsymbol{X}}$ of the next time step, and returns to step (2);

(5) The algorithm completes the tracking control process and ends the calculation.

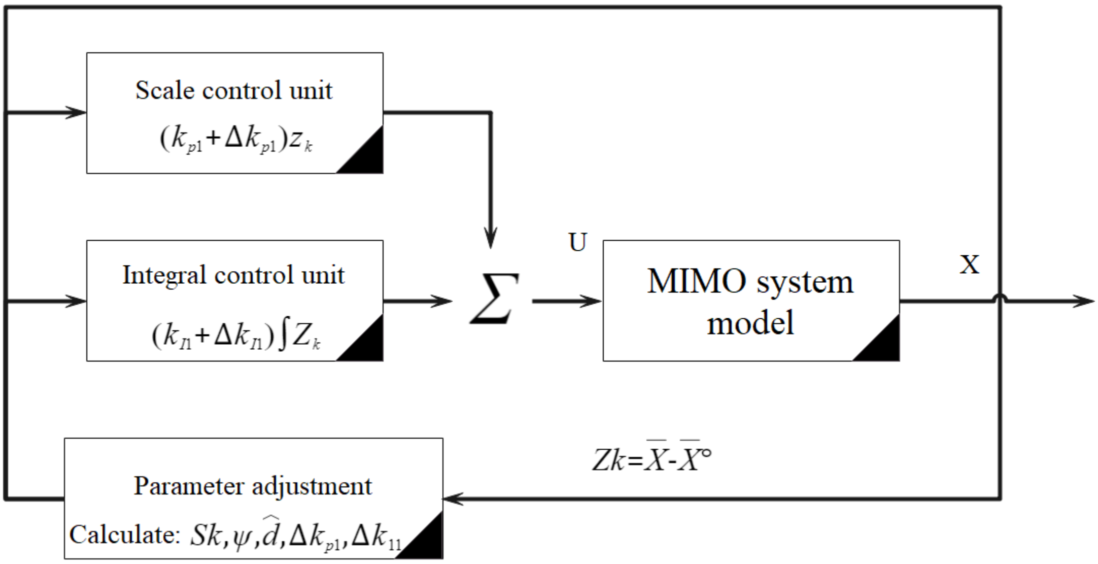

Figure 1 Control strategy algorithm block diagram

In order to further improve the accuracy of tracking control, for the described nonlinear system, iterative calculation can also be performed based on the idea of the iterative method to reduce the tracking control error.

Next, the complete failure of some actuators is considered. For this failure mode, new state vectors $\boldsymbol{Y}$ and $\overline{\boldsymbol{Y}}$ are introduced in the following form:

$$\boldsymbol{Y} = \boldsymbol{C}\boldsymbol{X}, \overline{\boldsymbol{Y}} = \boldsymbol{C}\overline{\boldsymbol{X}} \quad (22)$$

The new generalized tracking error $\boldsymbol{Z}_k$ and the corresponding filtering variable $\boldsymbol{S}_k$ are defined as follows:

$$\boldsymbol{Z}_k = \boldsymbol{C}\boldsymbol{Z}$$
$$\boldsymbol{S}_k = \boldsymbol{C}\boldsymbol{S} \quad (23)$$

According to formula (3), the relationship between the new filter variable S_k and the tracking error Z_k can be obtained:

$$\boldsymbol{S}_k = \boldsymbol{Z}_k + \beta \int_0^t \boldsymbol{Z}_k \quad (24)$$

Next, a generalized PI control strategy for complete failure of some actuators is proposed in the following form:

$$\boldsymbol{u} = -\frac{\boldsymbol{A}^T\boldsymbol{C}^T}{\|\boldsymbol{C}\boldsymbol{A}\|}(k_{P2} + \Delta k_{P2}(t))\boldsymbol{Z}_k(t)$$
$$-\frac{\boldsymbol{A}^T\boldsymbol{C}^T}{\|\boldsymbol{C}\boldsymbol{A}\|}(k_{I2} + \Delta k_{I2}(t)) \int_0^t \boldsymbol{Z}_k(t)d\tau \quad (25)$$

The above PI controller also has the characteristics of simple structure and low computational cost. The PI gain is determined by the following formula:

$$\Delta k_{P2}(t) = \sigma_1 \hat{d}\psi^2, \Delta k_{I2}(t) = \beta \Delta k_{P2}(t) \quad (26)$$

Among them,

$$\dot{\hat{d}} = -\sigma_0 \hat{d} + \sigma_1 \psi^2 \|\boldsymbol{S}_k\|^2, \hat{d}(0) \geq 0 \quad (27)$$

$d = b^2$ is also a newly defined parameter, which will be mentioned in a later article. $\hat{d}$ is an estimate of the parameter d, and the definitions of $\sigma_0 > 0$ and $\sigma_1 > 0$ are the same as before.

When considering the generalized tracking error and filter variables defined by formula (23), If the PI gain is automatically updated by the algorithms (26) and (27) under the control of the PI control strategy of formula (25), the eventually consistent and bounded stable tracking control of the system can be achieved.

Certification:

Using the filter variable S_k defined by formula (24), the control law of formula (25) can be re-expressed as follows:

$$\boldsymbol{u} = -\frac{\boldsymbol{A}^T\boldsymbol{C}^T}{\|\boldsymbol{CA}\|}(k_{P2} + \Delta k_{P2}(t))\boldsymbol{S}_k \quad (28)$$

Then the derivative of the filter variable S_k can be obtained:

$$\begin{aligned}\boldsymbol{S}_k &= \boldsymbol{Z}_k + \beta\boldsymbol{Z}\\ &= \mathbf{CA}Mpu + \mathbf{C}L + \beta\mathbf{CZ} \quad (29)\end{aligned}$$

We choose the Lyapunov function of the following form to prove the stability of the closed-loop system:

$$V_2 = \frac{1}{2}S_k^T S_k + \frac{1}{2v}\tilde{d}^2 \quad (30)$$

Among them, $\tilde{d} = d - v\hat{d}$ is an unknown estimation error parameter. Further, by derivation of the above formula, we can get:

$$\begin{aligned}\dot{V}_2 &= \boldsymbol{S}_k^T\dot{\boldsymbol{S}}_k + \frac{1}{v}\tilde{d}\dot{d}\\ &= \mathbf{S}_k^T(\boldsymbol{CAMu} + \boldsymbol{CL} + \beta\boldsymbol{CZ}_k) + \frac{1}{v}\tilde{d}(\dot{d} - \mu\dot{\hat{d}})\\ &= -\frac{k_{P2}+\Delta k_{P2}}{\|\boldsymbol{CA}\|}\boldsymbol{S}_k^T(\boldsymbol{CAM\rho A}^T\boldsymbol{C}^T)\boldsymbol{S}_k + \boldsymbol{S}_k^T(\boldsymbol{CL} + \beta\boldsymbol{CZ}) - \tilde{d}\dot{\hat{d}} \quad (31)\end{aligned}$$

Further, we get:

$$\begin{aligned}&-\frac{k_{P2} + \Delta k_{P2}}{\|\boldsymbol{CA}\|}\boldsymbol{S}_k^T(\boldsymbol{CAM\rho A}^T\boldsymbol{C}^T)\boldsymbol{S}_k\\ &= -\frac{k_{P2} + \Delta k_{P2}}{\|\boldsymbol{CA}\|}\boldsymbol{S}_k^T\begin{bmatrix}\frac{\boldsymbol{CAM\rho A}^T\boldsymbol{C}^T + (\boldsymbol{CAM\rho A}^T\boldsymbol{C}^T)^T}{2}\\ +\frac{\boldsymbol{CAM\rho A}^T\boldsymbol{C}^T - (\boldsymbol{CAM\rho A}^T\boldsymbol{C}^T)^T}{2}\end{bmatrix}\\ &= -\frac{k_{P2} + \Delta k_{P2}}{\|\boldsymbol{CA}\|}\boldsymbol{S}_k^T\frac{\boldsymbol{CAM\rho A}^T\boldsymbol{C}^T - (\boldsymbol{CAM\rho A}^T\boldsymbol{C}^T)^T}{2}\boldsymbol{S}_k\\ &\leq -(k_{P2} + \Delta k_{P2})v\|\boldsymbol{S}_k\|^2\\ &= -k_{P2}v\|\boldsymbol{S}_k\|^2 - \sigma_1 v\hat{d}\psi^2\|\boldsymbol{S}_k\|^2 \quad (32)\end{aligned}$$

Similarly, the above formula applies the properties of antisymmetric matrices:

$$\boldsymbol{S}_k^T\left[\frac{\boldsymbol{CAM\rho A}^T\boldsymbol{C}^T - (\boldsymbol{CAM\rho A}^T\boldsymbol{C}^T)^T}{2}\right]\boldsymbol{S}_k = 0 \quad (33)$$

According to the assumption, it can be further obtained:

$$\begin{aligned}\|\boldsymbol{CL} + \beta\boldsymbol{CZ}\| &\leq \|\boldsymbol{C}(\boldsymbol{L} + \beta\boldsymbol{Z})\|\\ &\leq \|\mathbf{C}\|\|\mathbf{L} + \beta\mathbf{Z}\|\\ &\leq a\|\mathbf{C}\|\psi(\cdot) = b\psi(\cdot) \quad (34)\end{aligned}$$

Among them, $b = a\|\boldsymbol{C}\|, a$ and $\psi(\cdot)$are defined above.

On this basis, we further get:

$$\boldsymbol{S}_k^T(\boldsymbol{CL} + \beta\boldsymbol{CZ}) \leq b\psi\|\boldsymbol{S}_k\| \leq \frac{1}{4\sigma_1} + \sigma_1 d\psi^2\|\boldsymbol{S}_k\|^2 \quad (35)$$

From formulas (31)-(35), there are the following inequalities:

$$\begin{aligned}\dot{V}_2 \leq& -k_{P2}v\|\boldsymbol{S}_k\|^2 - \sigma_1 v\hat{d}\psi^2\|\boldsymbol{S}_k\|^2\\ &+\frac{1}{4\sigma_1} + \sigma_1 d\psi^2\|\boldsymbol{S}_k\|^2 + \sigma_0\tilde{d}\hat{d} - \sigma_1\tilde{d}\psi^2\|\boldsymbol{S}_k\|^2\end{aligned}$$

$$= -k_{P2}v\|\boldsymbol{S}_k\|^2 + \sigma_1(d - v\hat{d})\psi^2\|\boldsymbol{S}_k\|^2$$
$$- \sigma_1\tilde{d}\psi^2\|\boldsymbol{S}_k\|^2 + \frac{1}{4\sigma_1} + \sigma_0\tilde{d}\hat{d}$$
$$= k_{P2}v\|\boldsymbol{S}_k\|^2 + \frac{1}{4\sigma_1} + \sigma_0\tilde{d}\hat{d} \quad (36)$$

When applying Young's inequality to the above equation, $\sigma_0\tilde{d}\hat{d}$ satisfies:

$$\sigma_0\tilde{d}\hat{d} = \sigma_0\tilde{d}\frac{1}{v}(d - \tilde{d})$$
$$\leq \frac{\sigma_0}{v}\tilde{d}d - \tilde{d}^2$$
$$\leq \frac{\sigma_0}{v}\left(\frac{1}{2}\tilde{d}^2 + \frac{1}{2}d^2 - \tilde{d}^2\right)$$
$$= \frac{\sigma_0}{2v}d^2 - \frac{\sigma_0}{2v}\hat{d}^2 \quad (37)$$

By substituting formula (37) into formula (36), we can get:

$$\dot{V}_2 \leq k_{P2}v\|\boldsymbol{S}_k\|^2 - \frac{\sigma_0}{2v}\hat{d}^2 + \frac{1}{4\sigma_1} + \frac{\sigma_0}{2v}d^2$$
$$\leq -l_3V_2 + l_4 \quad (38)$$

Among them,

$$l_3 = min\{2k_{P2}v, \sigma_0\}, l_4 = \frac{1}{4\sigma_1} + \frac{\sigma_0}{2v}d^2 \quad (39)$$

Further, formula (38) can be further expressed as:

$$\dot{V}_2 \leq -k_{P2}v\|S_k\|^2 + l_4 \quad (40)$$

It means that $\|\boldsymbol{S}_k\|$ will enter the compact set:

$$\Omega_2 = \left\{\boldsymbol{S}_k \left\|\boldsymbol{S}_k \leq \sqrt{\frac{l_4+\eta_2}{k_{P2}v}}\right\|\right\} \quad (41)$$

Among them, $\eta_2 > 0$ is a small constant. The above formula shows that $S_k \in \ell_\infty$ is eventually uniformly bounded, so the newly defined generalized tracking error $\boldsymbol{Z}_k \in \ell_\infty$ also satisfies the eventually uniformly bounded condition. From this, the stability of the adaptive PI control strategy in the case of executive de-total failure is also demonstrated.

Similarly, the steps of adaptive fault-tolerant PI control for actuator complete failure mode are given, and its algorithm block diagram is shown in Figure 2:

(1) The algorithm sets the parameter σ_0、σ_1、ω_1、β、k_{P2} and gives the initial values $\hat{d}(0), \boldsymbol{Y}(0)$ and $\dot{\boldsymbol{Y}}(0)$;

(2) The algorithm calculates $\boldsymbol{Z}_k$、$\boldsymbol{S}_k$、ψ、$\hat{d}$ and obtains Δk_{P2} and Δk_{I2};

(3) The algorithm calculates the system input $\boldsymbol{u}$ according to the control law (25);

(4) The algorithm obtains the state quantities $\boldsymbol{Y}$ and $\dot{\boldsymbol{Y}}$ of the next time step, and returns to step (2);

(5) The algorithm completes the tracking control process and ends the calculation.

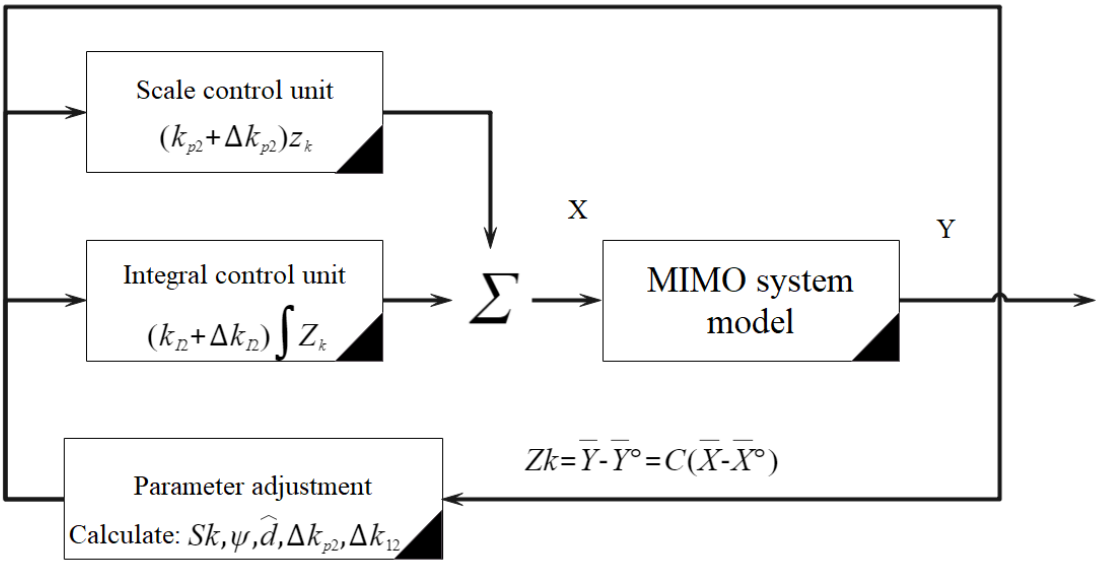

Figure 2 Control strategy algorithm block diagram

In order to verify the effectiveness and stability of the designed adaptive fault-tolerant PI control strategy, an iterative algorithm is used to improve the tracking control accuracy. For the failure mode of partial failure of the actuator, the formula is substituted into formula (11), and the dynamic equation of tourism demand under the failure mode can be obtained, and the form is as follows:

$$M\ddot{x}_1 = \boldsymbol{\kappa}(\rho\boldsymbol{u} + \boldsymbol{u}_r) - F_d(\cdot) - F_I(\cdot)$$
$$= \sum_{i=1}^{r} \kappa_i \rho_i u_i + \sum_{i=1}^{r} \kappa_i u_{ri} - F_d(\cdot) - F_I(\cdot) \quad (42)$$

The above formula can be sorted out to get a standard form of control model:

$$\ddot{x}_1 = \sum_{i=1}^{m} M^{-1}\kappa_i\rho_i u_i + \sum_{i=1}^{m} M^{-1}\kappa_i u_{ri} - M^{-1}F_d(\cdot) - M^{-1}F_I(\cdot)$$
$$= Gu + F(\cdot) \quad (43)$$

Among them,

$$G = M^{-1}\kappa\boldsymbol{\rho}$$
$$F(\cdot) = -M^{-1}F_d(\cdot) - M^{-1}F_I(\cdot) + M^{-1}\kappa u_r + d(\cdot) \quad (44)$$

On this basis, the displacement tracking error and velocity tracking error are defined as follows:

$$e = x_1 - x_1^*$$
$$\dot{e} = \dot{x}_1 - \dot{x}_1^* \quad (45)$$

Further, the generalized tracking error can be obtained:

$$Z = \omega_1 e + \dot{e} \quad (46)$$

Differentiating the above equation with respect to time and referring t, we can get:

$$\dot{Z} = \omega_1\dot{e} + \ddot{e} = \sum_{i=1}^{m} M^{-1}\kappa_i\rho_i u_i + L \quad (47)$$

Among them,

$$L = F(\cdot) + \omega_1\dot{e} - \ddot{x}_1^* \quad (48)$$

According to the control strategy, if Δk_{P1} and Δk_{I1} are automatically updated according to the definitions, then the tracking control for the position and speed of travel demand can be realized.

4 TOURISM DEMAND FORECAST BASED ON ADAPTIVE NEURAL NETWORK TECHNOLOGY IN BUSINESS INTELLIGENCE

Based on the self-adaptive algorithm research in the third part, this paper constructs a tourism demand forecasting model based on self-adaptive neural network technology. As lifestyle changes, predicting changes in traffic behavior requires the use of clearly activity-dependent models to study traveler's daily traffic behavior. Usually, it is necessary to focus on the connection state of an individual's activities in a day and transportation. Since people are restricted by working time, work place and obligations in the family, the activities of an individual in a day and transportation are relatively fixed. To analyze the travel behavior of people in a day, there are usually multiple trips, and daily travel can be regarded as a travel chain composed of multiple paths, and the base point of each travel path is not just home. According to different factors such as occupation and age, the travel chain varies greatly, and the traffic status always changes with time. This paper combines the time axis with the travel chain of people to form the interdependent relationship between the time, space and activities of people's activities. Moreover, this paper uses a three-dimensional prism-like space-time map to analyze the daily traffic behavior of people in a day, as shown in Figure 3.

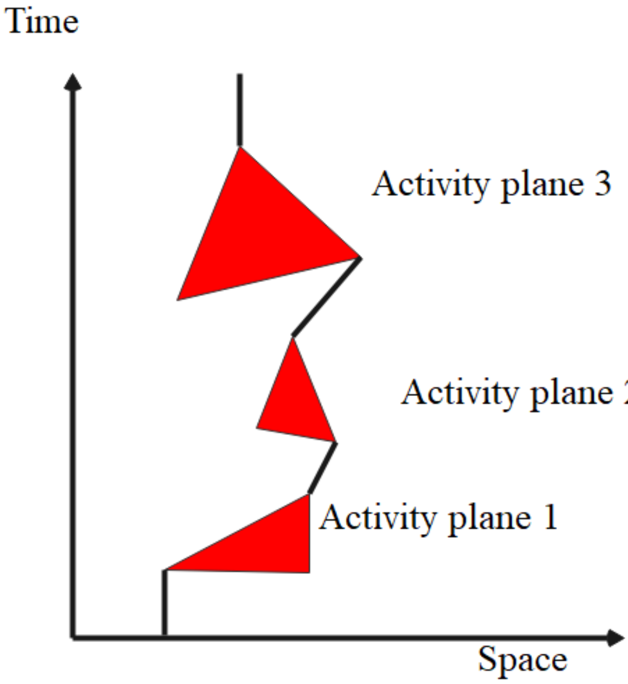

Figure 3. Time-space diagram of traffic behavior

For the analysis of tourism travel behavior, the time-space analysis is carried out by referring to the analysis method of daily traffic behavior. In the coordinate space composed of the city plane and the time axis, the expansion of tourists' possible activities in time and space can be represented by a prism. The characteristics of time and space analysis of tourism behavior are used in the connection and travel chain of activities and trips in the three-dimensional space introduced into the time axis, and the analysis is carried out focusing on the time constraints of tourism behavior and tributary time (travel time, tour time). It can be seen from the figure that the process of people's tourism behavior is the process of seeking the maximization of tourism utility under certain time constraints. t0 is the departure time from home, t5 is the time to return home, then t5-t0 is the maximum time of the entire trip. In the case of a fixed travel time range, the sightseeing time and the time spent on the journey are mutually restricted and distributed.

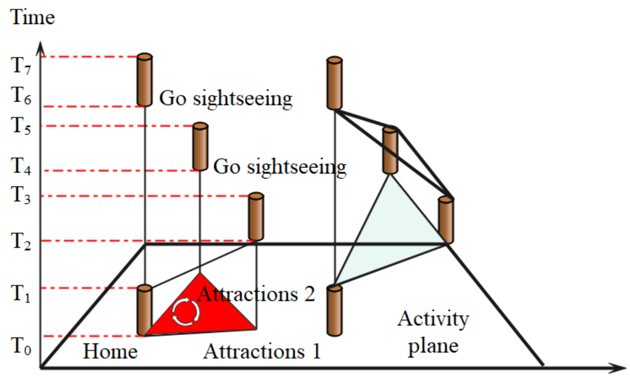

Figure 4 Spatial and temporal analysis of tourism travel behavior

Self-driving travel is an important part of social activities and a consumption behavior. Differences in people's travel needs also determine the changes in travel behavior. Due to the increased ability of high-income groups to pay for transportation consumption (such as fuel consumption, road transit fees, etc.), the demand for travel space for car owners has further increased. The space demand is not only the increase in the distance of self-driving out of the city, but also the increase in the driving distance of roaming activities in the tourist area after driving to the tourist destination. Also, people of different age groups hold different values of time. The time value of young and middle-aged people is bound to be higher than that of the elderly and young people. This group of people pays more attention to the efficiency of time use in the process of sightseeing and travel, especially the roaming process, and has higher requirements for the convenience of road traffic conditions.

The quantitative forecasting of tourism traffic demand is to predict the traffic demand of tourism travel activities under different development stages and different types of tourism destinations. Tourism traffic demand consists of two parts: tourism travel demand and tourism destination traffic demand. Tourism traffic demand is affected by socioeconomic factors, tourist destination capacity and facilities, service level, transportation mode characteristics, tourist destination attractiveness, transportation policy, external conditions and other factors, as shown in Figure 5.

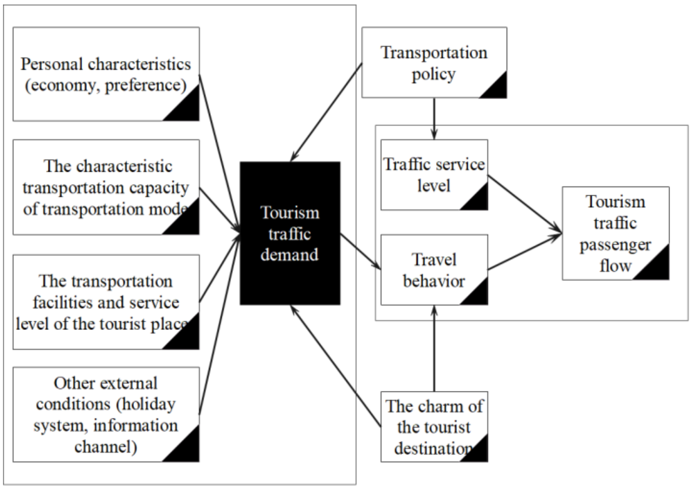

Figure 5 Characteristics of the traffic phenomenon in tourist areas

This paper uses the working mechanism of Boosting to construct the tourism demand forecasting model. The working mechanism of Boosting is shown in Figure 6. It first uses the original training set to train the first weak learner, and then adjusts the training set according to the performance of this weak learner to improve the attention of the wrongly predicted samples in subsequent training. Then, it trains the next weak learner based on the adjusted training set, and so on to obtain multiple weak learners. Finally, it combines these weak learners in a certain way to obtain a strong learner. The main difference between the algorithms is the adjustment of the training set and the combination of weak learners.

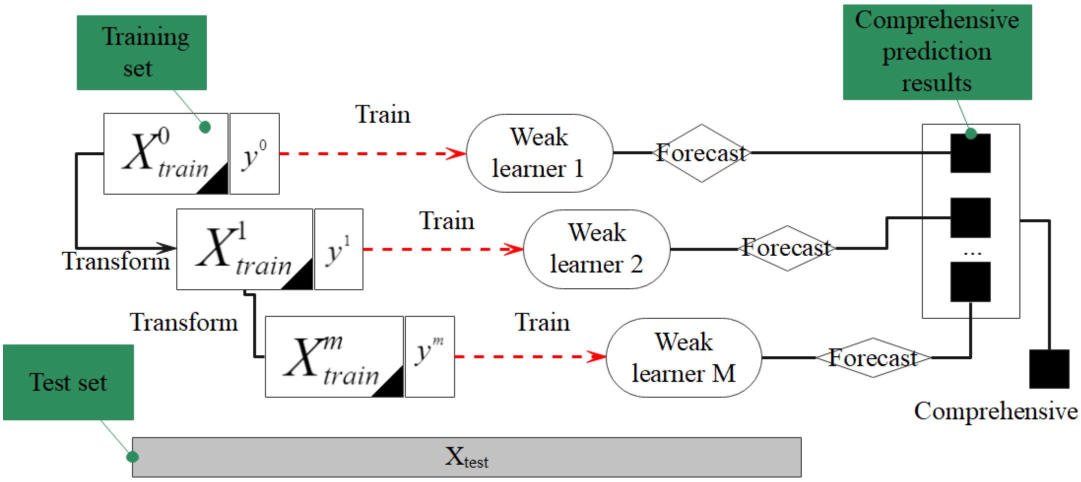

Figure 6 Boosting working mechanism

After tourists visit a stop point, they need to choose the next stop point to continue the tour. The transfer direction of tourists between stop points is affected by various factors, such as the state and attractiveness of the next stop point, and is also closely related to the guide signs of the scenic spot or the personal preference, cognitive ability, and social characteristics of tourists themselves. It takes a certain amount of time for tourists to move from one stop to another. Although the length of the path space between the stop points is a fixed value, the time it takes for tourists to pass the path is not a fixed value, which is closely related to the tourist rhythm and the mode of transportation they use. Moreover, the stay time of tourists at the stop point is also the time during which the stop point provides services for the tourists. The length of stay time is related to the function, attractiveness, tourist's own preference, physiological rhythm, etc. of the stop point, and should be dynamically determined accordingly.

Tourist travel rules are the way tourists follow to visit attractions. Tourists' tour rules include first-come-first-visit, last-come-last tour, priority tour and random tour. It also includes whether later tourists choose to wait in line or choose to visit other scenic spots when the capacity of the scenic spots is already saturated.

By integrating temporal geography with the theory of probabilistic temporal geography, system analysis theory, and tourist flow space-time bayonet theory, a research framework based on WITNESS simulation system to predict tourist flow spatio-temporal bayonet is proposed. Among them, temporal geography and probabilistic temporal geography provide a theoretical basis for establishing a probability-based scenic system simulation model. According to the system analysis theory, the scenic spot system is analyzed from the two aspects of the scenic spot environment and tourists' behavior rules, and the scenic spot environment is abstracted and simplified into three categories: entrance and exit, path and stop point. The tourist behavior rules are divided into tourist arrival rules, mobile stay rules and tour rules. According to the results of the system analysis, data about the spatial area, location layout, path length, and tourist arrival probability distribution, route transition probability, stay time probability distribution, and scenic spot moving time are collected according to the results of the system analysis. It provides initial parameters for the probability-based simulation system model and implements the model on the WITNESS simulation software platform. Finally, according to the tourist flow spatiotemporal bayonet theory, the paper proposes the tourist flow spatiotemporal density index as an index to identify the tourist flow spatiotemporal bayonet. The proposed research framework can provide reference and guidance for establishing the same simulation model for other types of scenic spots to predict the time-space checkpoint of tourism flow, as shown in Figure 7.

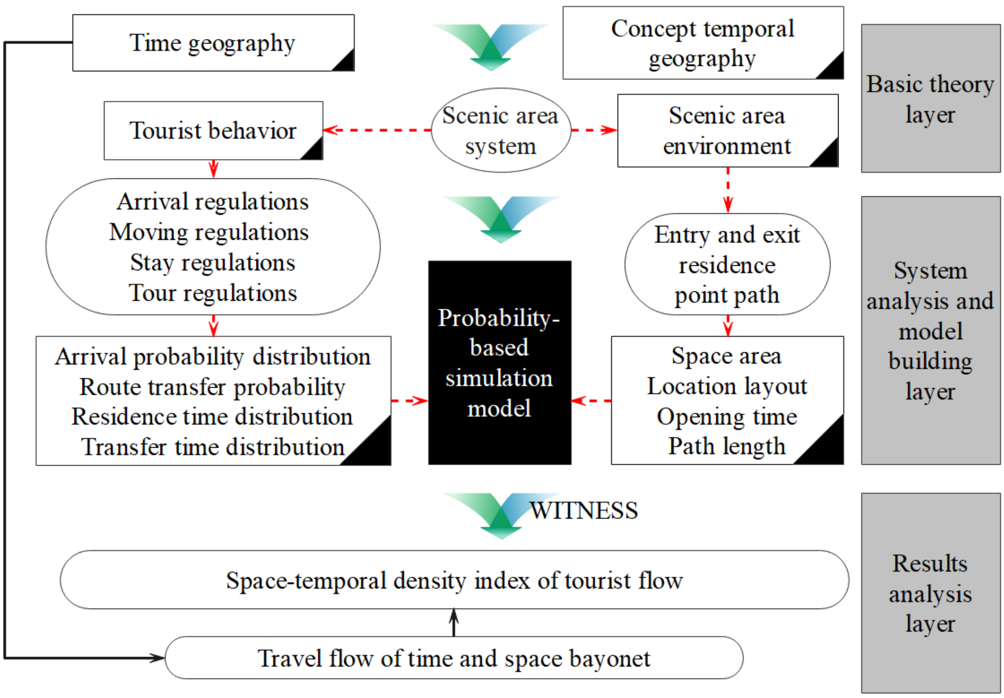

Figure7 The research framework for predicting the spatiotemporal bayonet of tourism flow based on the WITNESS simulation system

On the basis of the above research, the model in this paper is tested. The two-dimensional forward normal cloud generator generates the following two-dimensional cloud distribution cloud figure 8. It can be seen from figure 8 that the intelligent tourism demand forecasting system proposed in this paper has a strong function of forecasting data processing.

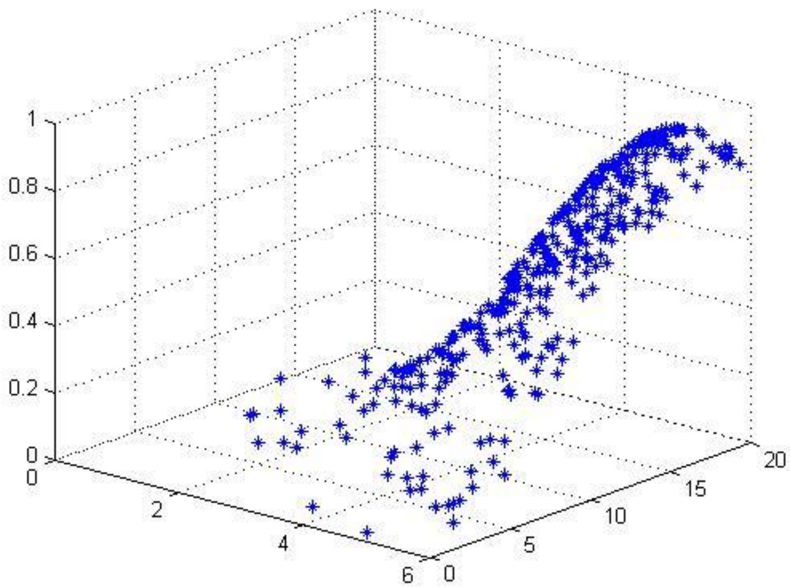

Figure 8. Two-dimensional cloud distribution map satisfying numerical characteristics

On the basis of the above research, the effect of the tourism demand forecasting model based on adaptive neural network technology proposed in this paper is evaluated, and the results of multiple groups of forecasting are counted, as shown in Table 1.

Table 1 Tourism forecasting effect of tourism demand forecasting model based on adaptive neural network technology

Num	Prediction effect	Num	Prediction effect	Num	Prediction effect
1	93.27	24	93.61	47	89.02
2	90.53	25	93.66	48	88.24
3	92.50	26	91.39	49	91.25
4	87.63	27	87.13	50	88.10
5	88.84	28	87.35	51	87.17
6	87.32	29	90.52	52	91.52
7	92.87	30	92.72	53	90.20
8	91.32	31	91.86	54	88.30
9	91.64	32	91.22	55	87.31
10	90.24	33	91.37	56	87.07
11	90.37	34	89.99	57	91.44
12	88.66	35	92.12	58	88.48
13	93.06	36	89.50	59	93.22
14	88.86	37	88.04	60	90.21
15	93.73	38	87.50	61	89.48
16	90.26	39	93.31	62	89.76
17	93.44	40	92.02	63	92.80
18	92.77	41	90.59	64	89.16
19	91.85	42	90.87	65	89.54
20	88.99	43	89.75	66	88.43
21	90.22	44	88.11	67	91.37
22	91.91	45	91.72	68	87.21
23	91.56	46	90.52	69	92.14

From the above research, it can be seen that the tourism demand forecasting model based on adaptive neural network technology proposed in this paper has a good tourism demand forecasting effect, and has a certain effect on promoting the development of tourism.

5 CONCLUSION

For cities, scenic spots, and hotels, planning and arrangements need to be adjusted according to factors such as off-peak seasons and passenger flow. Therefore, it is very important to accurately predict the tourism demand. At present, there are many tourism demand forecasting models, but the tourism demand forecasting models with high interpretability are more reliable and more likely to be adopted by relevant departments. For tourism planners, it is very important to explore the factors that most affect the overall planning of tourism. Therefore, it is necessary to find out the most important factors affecting the tourism volume through the interpretation of the model application, so as to formulate better tourism planning. This paper combines the adaptive neural network technology to construct the demand forecasting model. The experimental research shows that the tourism demand forecasting model based on adaptive neural network technology proposed in this paper has a good tourism demand forecasting effect and plays a certain role in promoting the development of tourism.

REFERENCES

[1] Wang, R., Hao, J. X., Law, R., & Wang, J. (2019). Examining destination images from travel blogs: A big data analytical approach using latent Dirichlet allocation. Asia Pacific Journal of Tourism Research, 24(11), 1092-1107.

[2] Wang, C. J., Ng, C. Y., & Brook, R. H. (2020). Response to COVID-19 in Taiwan: big data analytics, new technology, and proactive testing. Jama, 323(14), 1341-1342.

[3] Llorca, C., Molloy, J., Ji, J., & Moeckel, R. (2018). Estimation of a long-distance travel demand model using trip surveys, location-based big data, and trip planning services. Transportation Research Record, 2672(47), 103-113.

[4] Zhu, L., Yu, F. R., Wang, Y., Ning, B., & Tang, T. (2018). Big data analytics in intelligent transportation systems: A survey. IEEE Transactions on Intelligent Transportation Systems, 20(1), 383-398.

[5] Juanjuan, Z. H. A. O., Chengzhong, X. U., & Tianhui, M. E. N. G. (2019). Big Data-Driven Residents' Travel Mode Choice: A Research Overview. ZTE Communications, 17(3), 9-14.

[6] Bulchand-Gidumal, J. (2021). M. Sigala, R. Rahimi, M. Thelwall (Eds.):"Big Data and Innovation in Tourism, Travel, and Hospitality. Managerial Approaches, Techniques, and Applications". Zeitschrift für Tourismuswissenschaft, 13(2), 309-310.

[7] Gallego, I., & Font, X. (2021). Changes in air passenger demand as a result of the COVID-19 crisis: Using Big Data to inform tourism policy. Journal of Sustainable Tourism, 29(9), 1470-1489.

[8] Anda, C., Erath, A., & Fourie, P. J. (2017). Transport modelling in the age of big data. International Journal of Urban Sciences, 21(sup1), 19-42.

[9] Han, Y., & Kim, Y. (2017). A study of measuring traffic congestion for urban network using average link travel time based on DTG big data. The Journal of The Korea Institute of Intelligent Transport Systems, 16(5), 72-84.

[10] FUKUDA, D. (2019). Innovative Travel Survey Methods and Behavior Modeling in the Era of Big Data. Asian Transport Studies, 5(3), 436-438.

[11] Alaei, A. R., Becken, S., & Stantic, B. (2019). Sentiment analysis in tourism: capitalizing on big data. Journal of Travel Research, 58(2), 175-191.

[12] Li, T., Wang, J., Huang, J., & Gao, X. (2020). Exploring temporal heterogeneity in an intercity travel network: A comparative study between weekdays and holidays in China. Journal of Geographical Sciences, 30(12), 1943-1962.

[13] Chen, M., Yang, J., Hu, L., Hossain, M. S., & Muhammad, G. (2018). Urban healthcare big data system based on crowdsourced and cloud-based air quality indicators. IEEE Communications Magazine, 56(11), 14-20.

[14] Del Vecchio, P., Mele, G., Ndou, V., & Secundo, G. (2018). Creating value from social big data: Implications for smart tourism destinations. Information Processing & Management, 54(5), 847-860.

[15] Wang, H., Tang, X., Kuo, Y. H., Kifer, D., & Li, Z. (2019). A simple baseline for travel time estimation using large-scale trip data. ACM Transactions on Intelligent Systems and Technology (TIST), 10(2), 1-22.

[16] Li, B., Kisacikoglu, M. C., Liu, C., Singh, N., & Erol-Kantarci, M. (2017). Big data analytics for electric vehicle integration in green smart cities. IEEE Communications Magazine, 55(11), 19-25.

[17] Tian, H., Presa-Reyes, M., Tao, Y., Wang, T., Pouyanfar, S., Miguel, A., ... & Iyengar, S. S. (2021). Data Analytics for Air Travel Data: A Survey and New Perspectives. ACM Computing Surveys (CSUR), 54(8), 1-35.

[18] Peak, C. M., Wesolowski, A., zu Erbach-Schoenberg, E., Tatem, A. J., Wetter, E., Lu, X., ... & Bengtsson, L. (2018). Population mobility reductions associated with travel restrictions during the Ebola epidemic in Sierra Leone: use of mobile phone data. International journal of epidemiology, 47(5), 1562-1570.

[19] Torre-Bastida, A. I., Del Ser, J., Laña, I., Ilardia, M., Bilbao, M. N., & Campos-Cordobés, S. (2018). Big Data for transportation and mobility: recent advances, trends and challenges. IET Intelligent Transport Systems, 12(8), 742-755.

[20] Chen, F., Zhang, J., Wang, Z., Shi, S., & Liu, H. (2019). Passenger travel characteristics and bus operational states: a study based on IC card and GPS data in Yinchuan, China. Transportation Planning and Technology, 42(8), 825-847.